# Nanoscopic insights into seeding mechanisms and toxicity of α-synuclein species in neurons

Dorothea Pinotsi[1+], Claire H. Michel[1+], Alexander K. Buell[2], Romain F. Laine[1], Pierre Mahou[1], Christopher M. Dobson[2], Clemens F. Kaminski[1], Gabriele S. Kaminski Schierle[1*]

[1]Department of Chemical Engineering and Biotechnology, University of Cambridge, Cambridge, Pembroke Street, Cambridge CB2 3RA, United Kingdom.

[2]Department of Chemistry, University of Cambridge, Cambridge, Lensfield Road, Cambridge CB2 1EW, United Kingdom

* To whom correspondence should be addressed. E-mail: gsk20@cam.ac.uk.

[+] contributed equally

**Keywords: optical nanoscopy, seeding, neurodegenerative disease, prion-like behaviour, α-synuclein**

**Abstract:**

**New strategies for visualizing self-assembly at the nanoscale level are prone to grant deep insights into the function and dysfunction of molecular machineries in cells and living organisms. Of particular interest is the self-assembly of misfolded proteins into amyloid fibrils, which is related to a range of neurodegenerative disorders, such as Alzheimer's and Parkinson's diseases. Here, we probe the links between the mechanism of α-synuclein aggregation and its associated neuronal toxicity by using optical nanoscopy directly in a neuronal cell culture model of Parkinson's disease. The nanoscale level of detail revealed by super-resolution microscopy enables us to show that amyloid fibrils of the protein are taken up by neuronal cells and act as seeds for elongation reactions which both consume endogenous α-synuclein and suppress its de novo aggregation. When α-synuclein is internalized in its monomeric form, however, it nucleates and triggers the aggregation of endogenous α-synuclein, leading to apoptosis, although there are no detectable cross-reactions between externally added and endogenous protein species. Monomer-induced apoptosis can be reduced by pre-treatment with seed fibrils, suggesting that partial consumption of the externally added or excess soluble α-synuclein can be significantly neuroprotective.**

\body

The proliferation of α-synuclein (AS) aggregates (1–6), including the existence of distinct 'prion-like' strains (7, 8) as well as their spatial propagation throughout the brain (9), have been proposed to occur in the brains of patients suffering from Parkinson's disease (PD) but their links to pathology and to neuronal death have remained elusive (10–13). In this study, we use optical nanoscopy (14–18) to observe neurons directly and to assay AS internalization, as well as fibril-induced templating reactions involving endogenous AS at the molecular level. We further correlate this information with toxic phenotypes.

We have previously shown that the presence of AS ''seed fibrils'' or ''seeds'', short fibrils, pre-formed *in vitro* (see Fig. 1 and Materials and Methods section) favors elongation reactions over spontaneous nucleation (term used for seed-independent aggregation hereafter) *in vitro* (18). Furthermore, the seed fibrils were found to display highly inhomogeneous growth kinetics, with a significant fraction showing little or no growth at all (18). Here, we use two-color *direct* stochastic optical reconstruction microscopy (*d*STORM), a super-resolution imaging method (14), to investigate how such processes may be modified in the cellular environment. The results show the potential of this technique for studying the mechanisms of aggregation events *in vivo* and provide evidence for the neuroprotective role of reducing the concentration of free AS in the cellular environment.

**Results and Discussion**

**Externally added seed fibrils of α-synuclein act as templates for exogenously added monomeric α-synuclein and prevent its nucleation.** We first incubated neuronal cells with AS seed fibrils (50 nM, 5% covalently labeled with Alexa Fluor 568 (AF568), green) and AS monomers (500 nM, 10% covalently labeled with Alexa Fluor 647 (AF647), red), either each individually, or both in sequence. Either seed fibrils and/or monomeric protein were taken up by cells within 1 h (Suppl. Fig. 1). Two-color *d*STORM imaging permitted us to distinguish between seed species and their subsequent elongation by monomer addition (see Suppl. Info for details). When cells were incubated with monomer only, we found that spontaneous aggregate formation by monomeric AS within cells occurs faster than *in vitro* (Fig. 2a and c) where aggregation proceeds slowly in the absence of mechanical agitation and/or surfaces that induce primary nucleation (19, 20). This observation suggests that within a cellular environment catalytically active surfaces, such as e.g. lipid bilayers (20) or low pH in endosomes (21) enhance the nucleation rate of AS. In the presence of both monomers and seed fibrils however (Fig. 2b), the

elongation of the latter *via* monomer addition dominates over spontaneous formation of aggregates. Indeed, *d*STORM experiments performed in SH-SY5Y cells show that the majority of added monomeric AS (red) is sequestered by the added AS seeds (green) (Fig. 2b and d). In particular, Fig. 2d shows a comparison between the lengths of aggregates formed by nucleation of exogenously added monomeric protein when this is added together with seed fibrils (red triangles-indicated by arrowheads in Fig. 3b) and the extent of seed elongation by exogenously added monomeric protein (dark blue squares-indicated by arrows in Fig. 3b). In order to quantify seed fibril elongation by added monomeric AS, we analyzed the length distributions of the species observed in each of the two detection channels (''red'' for monomer and ''green'' for seed fibrils) separately. We applied masks to imaged areas in which ''green'' and ''red'' signals co-localized and subsequently quantified the length of the red aggregates, which had elongated the seed fibrils. Similarly, in order to quantify the nucleation of added monomeric protein, we measured the length of the aggregates of the red channel which did not co-localize with any green seed fibrils (see Materials and Methods for details). Due to the high spatial resolution of *d*STORM imaging, we were able to distinguish between these two types of aggregation processes.

**Seed fibril elongation dominates over nucleation of endogenous AS.** In a next step we investigated whether or not exogenously added AS seed fibrils can be elongated by the endogenous AS present in dopaminergic neurons. We incubated both ventral-mesencephalic (VM) and SH-SY5Y cells with labeled AS seeds (50 nM, 5% covalently labeled with AF568, green) for 1 h before washing and incubating the cells in AS-free medium for 24 h. The neurons were then fixed and stained with primary antibodies against endogenous AS for either VM or SH-SY5Y cells, followed by a secondary AF647-labeled antibody. The *d*STORM images (Fig. 3) show that the exogenously added seed fibrils (green) are elongated through the addition of endogenous AS (red). We refer to the ensuing fibrillar species as hetero-fibrils (Fig. 3b and c) in both VM and SH-SY5Y cells. Moreover, we have measured seed elongation by comparing the size of seed fibrils *in vitro* with fibrils that were present in cells after 24h incubation in AS-free medium using TEM and obtain similar results as described above using super-resolution imaging (see Suppl. Fig. 3 and Suppl. Information for details).

A comparison of the lengths of endogenous AS aggregates, which do not co-localize with seeds and must therefore have formed by spontaneous nucleation ("Nucleation'' in Fig. 3d), with those which form the elongated segment of the added seed fibrils, giving rise to hetero-fibrils ("Seed elongation'' in Fig. 3d) demonstrates that endogenous AS is preferentially recruited to elongate exogenous seeds rather than undergoing nucleation. The analysis of the length distributions for seed elongation and monomer nucleation was performed in a similar fashion as described earlier for seeded elongation by exogenously added monomer (see Materials and Methods section in SI). In order to examine the likelihood of random co-localization between objects in the red and green channels, we performed a quantitative co-clustering analysis using Ripley's K function (see Suppl. Info). The results in Suppl. Fig. 4 show that there is no random co-localization between seed fibrils and monomeric protein. On the contrary, there is a clear positive correlation between seeds and addition of monomer, suggesting that seed fibrils grow by elongation reactions.

Furthermore, we found that neither of the primary antibodies used displayed significant cross-reactivity with the labeled AS added exogenously. We compared the length of hetero-fibrils formed in cells with the length of the initial AF568-labeled seed fibrils measured *in vitro* by staining the latter with the same primary and secondary antibodies as used in cells (Suppl. Fig. 5). The average length of the hetero-fibrils in cells was significantly greater than that of the initial seed fibrils. Overall, these data suggest that in neurons the rate of monomer addition to a pre-formed seed fibril is significantly faster than that of spontaneous nucleation, for both exogenously added and endogenous monomeric protein.

**Monomeric, but not fibrillar AS, added exogenously to neurons induces apoptosis after 72 h.** Many studies have recently shown that smaller, oligomeric species of AS rather than mature fibrils induce toxicity (12, 13, 22–24). Here, we addressed directly whether or not seed fibrils that are capable of seeding endogenous AS can induce toxicity in neuronal cells, as some reports have suggested (8,

25, 26). Using an apoptosis detection assay (Fig. 4d and Suppl. Fig. 9) we show that adding unlabeled seed fibrils (either 50 nM or 500 nM) to neurons does not lead to significantly increased cell death within 72 h of incubation in AS-free medium in comparison to untreated control neurons. In contrast, we find that the addition of unlabeled monomeric AS (500 nM) leads to significantly increased levels of apoptosis in VM cells under similar experimental conditions (Fig. 4d and Suppl. Fig. 6 and 9), confirming reports that correlate increased levels of AS with disease pathology (27, 28).

**Exogenously added monomeric AS triggers the nucleation of endogenous AS.** To test whether or not exogenous monomeric AS induces toxicity *via* co-aggregation with endogenous AS, we added monomeric AF647-labeled AS (500 nM, 10% covalently labeled with AF647, red) to VM cells in the absence of seed fibrils. Using the same protocol as described above for the detection of hetero-fibrils in VM and SH-SY5Y cells we observed that aggregates of endogenous AS were formed throughout the cell, even in areas that were not in close proximity to incorporated exogenous protein. Moreover, *d*STORM imaging revealed that the mean area of endogenous AS particles (stained with a primary and a secondary antibody conjugated with AF568, green) formed in the presence of exogenously added monomer was significantly higher than that of endogenous AS species present in control cells that had not been treated with exogenous AS monomers (Fig. 4c). It thus appears that the endocytosed exogenous monomer triggers the aggregation of endogenous AS (Fig. 4a (iii)) without the two moieties coming necessarily into direct contact. Similar results were obtained for SH-SY5Y cells (Suppl. Fig. 7). However, as we have previously shown in Fig. 2, exogenously added monomeric AS self-nucleates and forms small aggregates inside the cells. It therefore remains to be determined whether or not the exogenously added monomeric protein upon formation of small aggregates, can indirectly trigger endogenous AS nucleation via other mechanisms such as cell stress, the production of oxidative species, or through a general loss of protein homeostasis. Overall, these findings therefore link the aggregation of endogenous AS induced indirectly by exogenous monomer with an increased toxicity.

**Endocytosed monomeric AS has a reduced propensity to seed endogenous AS compared to pre-formed AS fibrils.** Having established that seed fibrils can elongate via addition of monomeric AS, both externally added and endogenous, we investigated the growth propensity of aggregates formed by endocytosed monomeric protein. We find that these aggregates have a reduced propensity to seed endogenous AS relative to pre-formed AS seed fibrils. Indeed, in previous experiments performed *in vitro* (18) we observed a high level of heterogeneity in the elongation rates for individual AS fibrils within a given population. We thus hypothesized that aggregates formed of endogenous AS upon addition of exogenous monomer might correspond to non-fibrillar structures or fibrillar populations with low seeding propensity. To test this idea we treated VM cells for 1 h with AF647-labeled monomeric AS (red), incubated them in AS-free medium for either 3 or 7 days and then for 1 h in medium containing monomeric AF568-labeled AS (green). This procedure was followed by a 24 h incubation period in AS-free medium (see Suppl. Information for details). Subsequent *d*STORM imaging (Suppl. Fig. 8a and b) reveals little growth of AF647-labeled AS aggregates *via* addition of AF568-labeled monomer, despite the two being clearly co-localized. Most of the aggregates appear globular, with only a few featuring elongated, fibrillar shapes. Taken together with the *in vitro* data reported earlier, these findings are consistent with the concept of amyloid fibril structural polymorphism (5, 29), i.e. that aggregates of the same peptide can exhibit a variety of conformational structures. This observation is interesting in the light of recent reports demonstrating that fibrillar mouse explants do not in all cases induce seeding in non-transgenic mice (30) and in other animal models of disease (31–33). Furthermore, our results indicate that in addition to fibrillar AS species, soluble AS can readily aggregate following uptake by cells, a conclusion similar to that drawn from experiments with Tau in a cellular model of Alzheimer's disease (21).

**Apoptosis can be counteracted by the addition of seed fibrils prior to exposure to monomeric AS.** In a final set of experiments we found that upon pre-incubation of neurons with seed fibrils for 1 h prior to the addition of monomeric AS, apoptosis was reduced to the levels observed in control cells (Fig. 4d). These results indicate a direct correlation between the nucleation of endogenous AS and

apoptosis when exogenous monomeric AS is added to neurons alone, but not when seed fibrils are also present. It appears likely that free monomeric AS is rapidly sequestered by the added seed fibrils, thus reducing the levels of soluble protein and decreasing the propensity for *de novo* formation of aggregates. The process of transmission of toxicity-inducing species from cell to cell thus appears to be potentially more complex than the simple transmission of fibrillar aggregates.

In conclusion, we have established a nanoscopic assay to track aggregation processes directly in neuronal cells which provides for a powerful tool to probe the links between specific mechanisms of AS amyloid fibril self-assembly and toxicity. In particular, we have shown that exogenously added fibrils can seed endogenous AS and that subsequent elongation of seed fibrils dominates over nucleation of endogenous AS. Moreover, exogenously added monomeric AS triggers aggregation of endogenous AS, and monomeric, but not fibrillar, AS added exogenously to neurons induces apoptosis. The latter effect however, can be counteracted by the addition of seed fibrils prior to exposure to monomeric AS, which may prevent the formation of small toxic species by reducing the excess monomeric protein pool. Taken together, our data suggest that the level of soluble AS is crucial to the development of AS pathology and that the relative concentrations of the different forms of AS are likely to play key role in the spreading of disease.

## Materials and Methods

Wild-type human α-synuclein was recombinantly expressed and purified as described previously (19). Super-resolution imaging *in vitro* and in cells was performed using a *d*STORM microscopy setup based on a Nikon Eclipse TE 300 inverted wide-field microscope and a 100x, 1.49 NA TIRF (total internal reflection fluorescence) objective lens (Nikon, UK Ltd.) as described in (18). The experiments were performed on both neuroblastoma cell cultures and on Ventral Mesencephalic (VM) neurons, dissected from rat embryos. Details on all the experimental protocols, methods and data analysis can be found in the Supplementary Information.

## Acknowledgements

We thank Dr Q. Jeng and Dr A. Stephens for technical assistance and Dr J. Skepper for TEM imaging. This work was funded by grants from the U.K. Medical Research Council (MR/K015850/1 and MR/K02292X/1), Alzheimer's Research UK (ARUK-EG2012A-1), U.K. Engineering and Physical Sciences Research Council (EPSRC) (EP/H018301/1) and the Wellcome Trust (089703/Z/09/Z). D.P. wishes to acknowledge support from the Swiss National Science Foundation and the Wellcome Trust through personal fellowships. A.K.B thanks Magdalene College, Cambridge and the Leverhulme Trust for support.

## References

1. Prusiner SB, Scott MR, DeArmond SJ, Cohen FE (1998) Prion protein biology. *Cell* 93(3):337–48.
2. Chiti F, Dobson CM (2006) Protein misfolding, functional amyloid, and human disease. *Annu Rev Biochem* 75:333–66.
3. Aguzzi A, Rajendran L (2009) The transcellular spread of cytosolic amyloids, prions, and prionoids. *Neuron* 64(6):783–90.
4. Brundin P, Melki R, Kopito R (2010) Prion-like transmission of protein aggregates in neurodegenerative diseases. *Nat Rev Mol Cell Biol* 11(4):301–7.
5. Eisenberg D, Jucker M (2012) The amyloid state of proteins in human diseases. *Cell* 148(6):1188–203.
6. Jucker M, Walker LC (2013) Self-propagation of pathogenic protein aggregates in neurodegenerative diseases. *Nature* 501(7465):45–51.

7. Guo JL, et al. (2013) Distinct α-synuclein strains differentially promote tau inclusions in neurons. *Cell* 154(1):103–17.
8. Bousset L, et al. (2013) Structural and functional characterization of two alpha-synuclein strains. *Nat Commun* 4:2575.
9. Braak H, et al. Staging of brain pathology related to sporadic Parkinson's disease. *Neurobiol Aging* 24(2):197–211.
10. Goldberg MS, Lansbury PT (2000) Is there a cause-and-effect relationship between alpha-synuclein fibrillization and Parkinson's disease? *Nat Cell Biol* 2(7):E115–9.
11. Caughey B, Lansbury PT (2003) Protofibrils, pores, fibrils, and neurodegeneration: separating the responsible protein aggregates from the innocent bystanders. *Annu Rev Neurosci* 26:267–98.
12. Danzer KM, et al. (2007) Different species of alpha-synuclein oligomers induce calcium influx and seeding. *J Neurosci* 27(34):9220–32.
13. Winner B, et al. (2011) In vivo demonstration that alpha-synuclein oligomers are toxic. *Proc Natl Acad Sci U S A* 108(10):4194–9.
14. Heilemann M, et al. (2008) Subdiffraction-resolution fluorescence imaging with conventional fluorescent probes. *Angew Chem Int Ed Engl* 47(33):6172–6.
15. Van de Linde S, et al. (2011) Direct stochastic optical reconstruction microscopy with standard fluorescent probes. *Nat Protoc* 6(7):991–1009.
16. Kaminski Schierle GS, et al. (2011) In situ measurements of the formation and morphology of intracellular β-amyloid fibrils by super-resolution fluorescence imaging. *J Am Chem Soc* 133(33):12902–5.
17. Duim WC, Chen B, Frydman J, Moerner WE (2011) Sub-Diffraction Imaging of Huntingtin Protein Aggregates by Fluorescence Blink-Microscopy and Atomic Force Microscopy. *Chemphyschem*:2387 – 2390.
18. Pinotsi D, et al. (2014) Direct Observation of Heterogeneous Amyloid Fibril Growth Kinetics via Two-Color Super-Resolution Microscopy. *Nano Lett* 14(1):339–45.
19. Buell AK, et al. (2014) Solution conditions determine the relative importance of nucleation and growth processes in α-synuclein aggregation. *Proc Natl Acad Sci U S A* 111(21):7671–6.
20. Galvagnion C, et al. (2015) Lipid vesicles trigger α-synuclein aggregation by stimulating primary nucleation. *Nat Chem Biol* 11(3):229–34.
21. Michel CH, et al. (2014) Extracellular monomeric tau protein is sufficient to initiate the spread of tau protein pathology. *J Biol Chem* 289(2):956–67.
22. Laganowsky A, et al. (2012) Atomic view of a toxic amyloid small oligomer. *Science* 335(6073):1228–31.
23. Celej MS, et al. (2012) Toxic prefibrillar α-synuclein amyloid oligomers adopt a distinctive antiparallel β-sheet structure. *Biochem J* 443(3):719–26.
24. Cremades N, et al. (2012) Direct observation of the interconversion of normal and toxic forms of α-synuclein. *Cell* 149(5):1048–59.
25. Pieri L, Madiona K, Bousset L, Melki R (2012) Fibrillar α-synuclein and huntingtin exon 1 assemblies are toxic to the cells. *Biophys J* 102(12):2894–905.
26. Peelaerts W, et al. (2015) α-Synuclein strains cause distinct synucleinopathies after local and systemic administration. *Nature* 522(7556):340–4.
27. Ahn T-B, et al. (2008) alpha-Synuclein gene duplication is present in sporadic Parkinson disease. *Neurology* 70(1):43–9.
28. Singleton AB, et al. (2003) alpha-Synuclein locus triplication causes Parkinson's disease. *Science* 302(5646):841.
29. Toyama BH, Weissman JS (2011) Amyloid structure: conformational diversity and consequences. *Annu Rev Biochem* 80:557–85.
30. Sacino AN, et al. (2014) Amyloidogenic α-synuclein seeds do not invariably induce rapid, widespread pathology in mice. *Acta Neuropathol* 127(5):645–65.
31. Brundin P, Li J-Y, Holton JL, Lindvall O, Revesz T (2008) Research in motion: the enigma of Parkinson's disease pathology spread. *Nat Rev Neurosci* 9(10):741–5.
32. Desplats P, et al. (2009) Inclusion formation and neuronal cell death through neuron-to-neuron transmission of alpha-synuclein. *Proc Natl Acad Sci U S A* 106(31):13010–5.
33. Kordower JH, et al. (2011) Transfer of host-derived α synuclein to grafted dopaminergic neurons in rat. *Neurobiol Dis* 43(3):552–7.

## Figures:

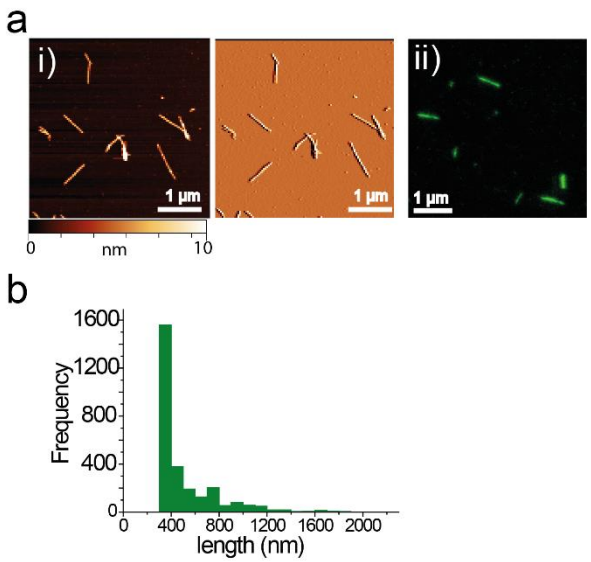


***Figure 1:*** *a) i) AFM (height and topographic profile) and ii) dSTORM images of AS seed fibrils labeled with AF568, formed and imaged in vitro, prior to addition to neuronal cell cultures. b) Histogram depicting the length distribution of such seed fibrils, determined by dSTORM imaging.*

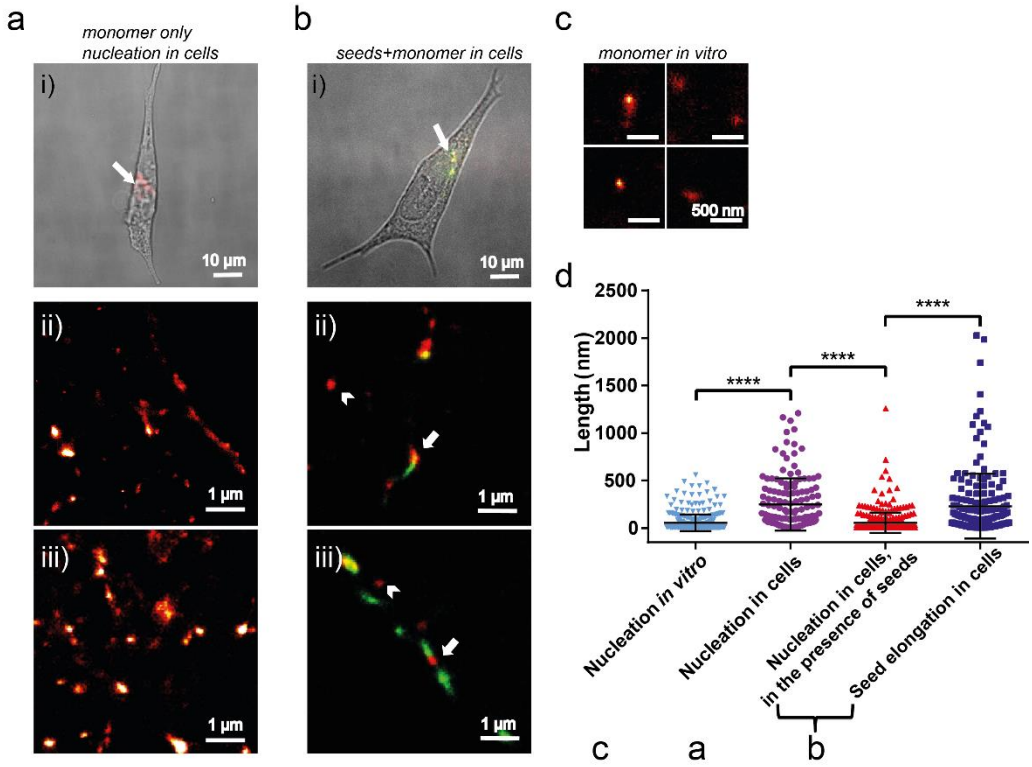


***Figure 2:*** *a) i) Overlaid differential interference contrast (DIC) and conventional fluorescence image of an SH-SY5Y cell treated for 1 h with AF647-labeled (red) AS monomer followed by a 24 h incubation in AS-free medium. a) ii) and iii) Zoomed-in dSTORM images showing the nucleation of monomeric AS inside neuronal cells, after incubation for 1 h followed by incubation for 24 h in AS-free medium. Scale bars: 1 µm. The image in (a)(ii) corresponds to the aggregates in the area indicated by the white arrow in (a)(i). b) i) Overlaid DIC and conventional fluorescence image of an SH-SY5Y cell treated for 1 h with AF568-labeled (green) AS seeds and then for 1 h with AF647-labeled (red) AS monomers followed by a 24 h incubation in AS-free medium. b) ii) and iii) Zoomed-in dSTORM images showing the seeds elongated by exogenously added monomeric AS, after 24 h incubation in AS-free medium (red, indicated by an arrow). Scale bars: 1 µm. The image in (b)(ii) corresponds to fibrils in the area indicated by the white arrow in (b)(i). c) Panels depicting different dSTORM images of monomeric AS after 24 h of incubation in vitro: no aggregation is observed. Scale bars: 500 nm. d) Quantification of the lengths of different AS species observed: monomeric AS after 24 h of incubation in vitro (light blue inverse triangles, panel c), aggregates formed of added monomeric AS after 24 h of incubation in cells that had been treated with monomeric AS only (purple circles, panel a), aggregates of added monomeric protein (AF647-labeled) in cells that do not co-localize with seeds after 24 h and indicated by an arrowhead in (b)(ii) and (iii) (red triangles, panel b), and the extent of seed elongation by addition of monomeric protein (AF647-labeled) in cells treated consecutively with seeds and monomeric AS after 24 h and indicated by an arrow in (b)(ii) and (iii) (dark blue squares, panel b). The statistical*

*analysis was performed using a one-way ANOVA: F(2, 713)=48.31 followed by a Tukey's multiple comparison test. ****: p<0.0001.*

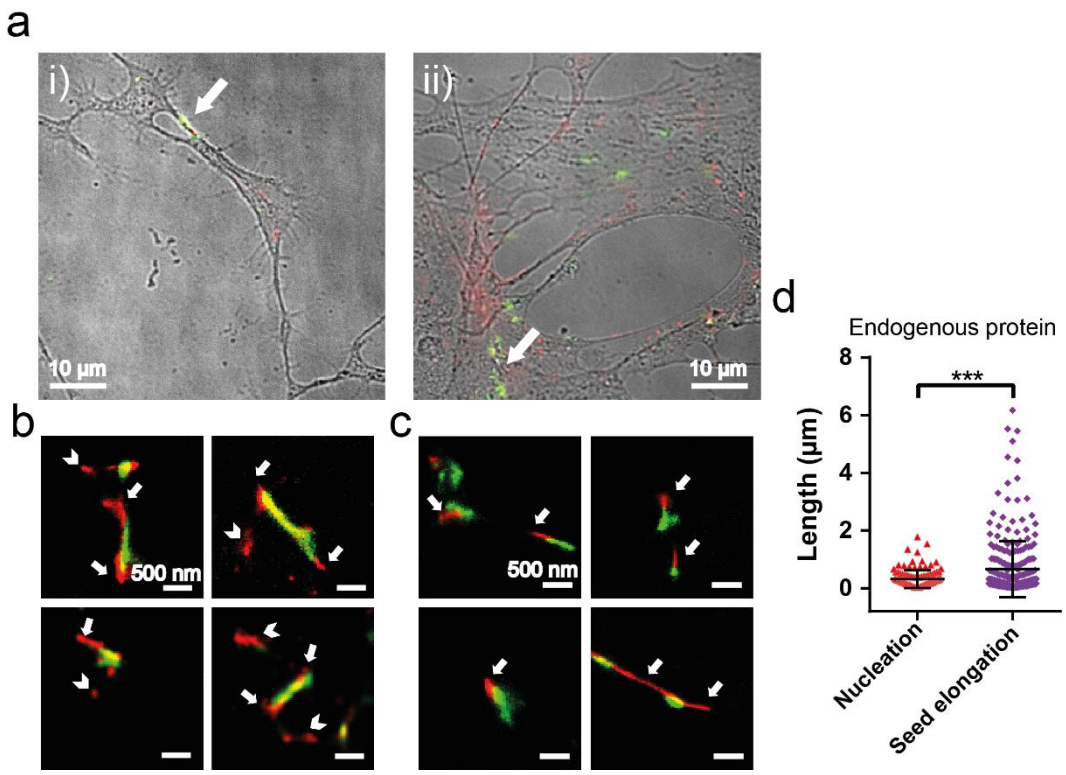


***Figure 3:*** *a) i) and ii) Overlaid DIC and wide-field fluorescence images of ventral-mesencephalic (VM) cells treated for 1 h with AF568-labeled AS seed fibrils (green), incubated for 24 h in AS-free medium and immunostained for endogenous AS with a secondary antibody tagged with AF647 (red). b) Zoomed-in dSTORM images of hetero-fibrils formed of exogenous seeds (green) elongated by endogenous AS (red, indicated by an arrow) in VM cells. The top two images correspond to fibrils located in the areas indicated by the white arrows in (a). Scale bars correspond to 500 nm. c) Zoomed-in dSTORM images of hetero-fibrils formed of exogenous seeds (green) elongated by endogenous AS (red, indicated by an arrow) in SH-SY5Y cells. d) Quantification of the extent of seed elongation by endogenous AS, such as this indicated by an arrow in (b) and (c) ("Seed elongation") and of the size of aggregates consisting of endogenous AS only, as indicated by an arrowhead in (b) ("Nucleation"). The statistical analysis was performed using an unpaired t-test. ***: p<0.001. The experiment was repeated 8 times in SH-SY5Y cells and 7 times in primary VM cell cultures and for each experiment at least 8 randomly chosen areas on the glass coverslip were imaged.*

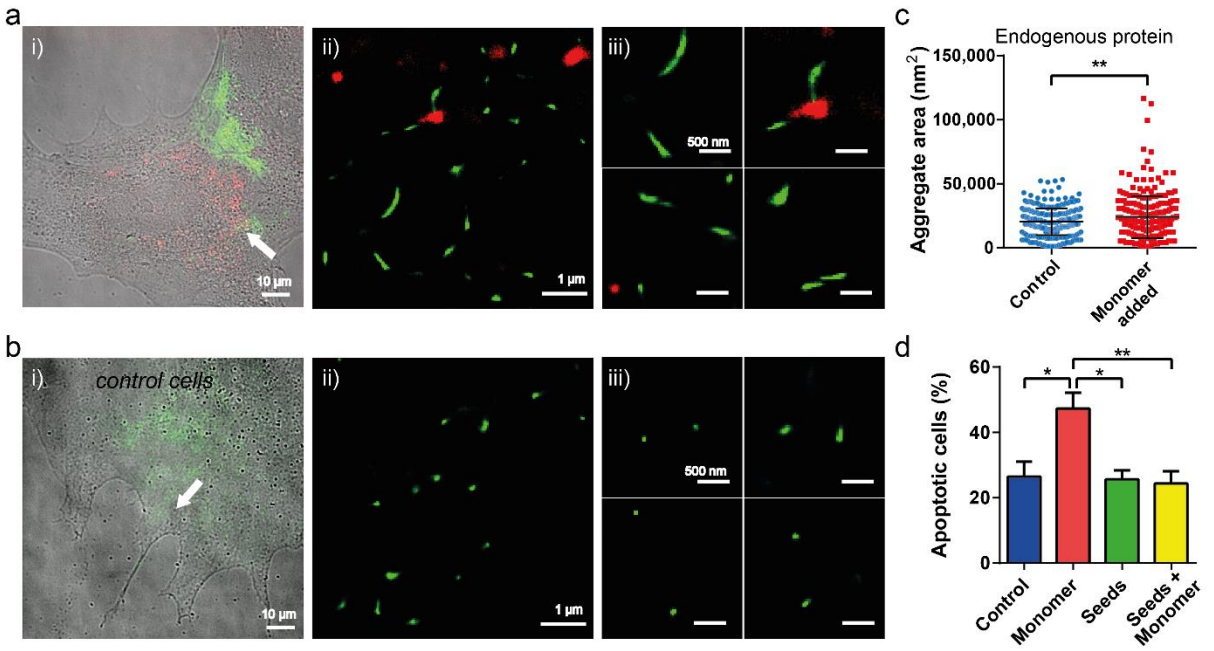


***Figure 4:*** *a) i) and b) i) Overlaid DIC and wide-field fluorescence images of VM cells immunostained for endogenous AS using a secondary antibody tagged with AF568 (green); either (a) treated for 1 h with monomeric AS labeled with AF647 (red), followed by a 24 h incubation in AS-free medium, or (b) untreated. a) ii) and b) ii) Zoomed-in dSTORM images in the areas indicated by white arrows. a) iii) and b) iii) Panels depicting zoomed-in dSTORM images of aggregates of the endogenous AS species (green) in both treated (a) and control cells (b); the scale bars indicate 500 nm. c) Size distribution of endogenous AS species formed in control cells compared with those in cells treated with monomeric AS. The statistical analysis was performed using an unpaired t-test. **: p<0.01. The experiment was repeated 7 times and for each time 10 randomly chosen areas were imaged at different locations on the glass coverslip. d) Percentage of apoptotic cells in control cells (blue), cells treated with monomer only (red), cells treated with seeds only (green) and cells treated consecutively with seeds and monomer (yellow). The statistical analysis was performed using a repeated measures ANOVA: F(3, 12) = 7.198 followed by a Tukey's multiple comparisons test. *: p<0.05; **:<0.01. The experiment was repeated 4 times and each time two samples per condition were analyzed.*